Applied Surface Science 363 (2016) 13–20

Contents lists available at ScienceDirect

Applied Surface Science

journal homepage: www.elsevier.com/locate/apsusc

Tailoring patterns of graphene wrinkles by circular torsion

Matthew Becton, Xianqiao Wang*

College of Engineering, University of Georgia, Athens, GA 30602, USA

ARTICLE INFO

Article history:
Received 31 July 2015
Received in revised form 17 October 2015
Accepted 7 November 2015
Available online 10 December 2015

Keywords:
Wrinkling
Graphene
Molecular dynamics
Torsion

ABSTRACT

Wrinkled graphene has been emerging as a hot topic of interest due to its easily induced physical changes accompanied by changes in its material behavior. However, the wrinkling pattern of graphene and its relevant properties remain poorly understood. Here we employ molecular dynamics simulations to model the behavior of graphene under periodic, torsional wrinkling and elucidate the effect of torsion pattern, torsion velocity, and hole size on the wrinkling characteristics of a large graphene sheet. Simulation results show that gross control over the wrinkling pattern is feasible via manipulation of torsion direction and relative hole size, with fine-tuning of the wrinkle formation possible by control of the relative torsion speed of each hole.

1. Introduction

For the past decade, graphene has been the subject of intensive study and research. Due to the many exemplary properties exhibited by this material graphene has demonstrated countless potential applications in electronics [1–4], energy storage [5,6], composites [7–9] and biomedicine [10–12] due to its outstanding thermal [13–15], mechanical [16], and electronic [17,18] properties. In these studies and applications, due to its flexible and 2D nature, graphene films are generally wrinkled or rippled with smooth undulations, and/or crumpled with sharp ridges, folds and vertices [19–22].

Many of the useful characteristics of graphene come from its extreme thinness and anisotropic morphology, such that investigations into both graphene and other 2D materials necessitate a certain focus on the material's associated geometry [23–25]. The nature of the unique functional abilities of graphene such as its electronic, magnetic, mechanical, and chemical properties is to a large extent determined by the morphology of the graphene sheet. Wrinkling of a 2-dimensional material induces multiple changes in its structure, and these changes can in turn affect the properties of the material [26–28]. As the deformation of graphene can strongly affect properties such as diffusion [29] and electrical conductivity [12,30], and thus has a notable effect on the performance of graphene-based devices and materials, the potentiality of wrinkling as a method to tailor the properties of graphene while maintaining film integrity is a topic of much interest [31–37]. It is anticipated that controllably tailoring the physical and electronic properties of 2D materials such as graphene using wrinkle patterns will better allow for multiple control methods in the development of novel or improved devices [38,39]. Thus it is necessary to properly investigate the patterns of wrinkles formed by deformation of graphene. In this work we investigate the effects of deliberate and methodical torsional straining on the wrinkle formation and patterns of a single crystal graphene sheet with periodic holes using nonequilibrium molecular dynamics.

2. Model and computational methods

Molecular dynamics simulations in this work are based on the open source code LAMMPS [40]. Periodic boundary conditions are employed to set up a pseudo-infinite simulation system, in order to mimic a large sheet. To better capture the behavior of the carbon surfaces we utilize the adaptive intermolecular reactive empirical bond order (AIREBO) potential for intra-graphene carbons as described by Stuart et al. [41] as

$$E = \frac{1}{2}\sum_{i}\sum_{j\neq i}\left[E_{ij}^{\mathrm{REBO}} + E_{ij}^{\mathrm{LJ}} + \sum_{k\neq i,jl\neq i,j,k}\sum E_{kijl}^{\mathrm{TORSION}}\right] \quad (1)$$

where the E_{ij}^{REBO} term is the REBO potential published by Brenner et al. [42], shown as

$$E_{ij}^{\mathrm{REBO}} = V_{ij}^{\mathrm{R}}(r_{ij}) + b_{ij}V_{ij}^{\mathrm{A}}(r_{ij}) \quad (2)$$

* Corresponding author.
E-mail address: xqwang@uga.edu (X. Wang).

http://dx.doi.org/10.1016/j.apsusc.2015.11.091
0169-4332/

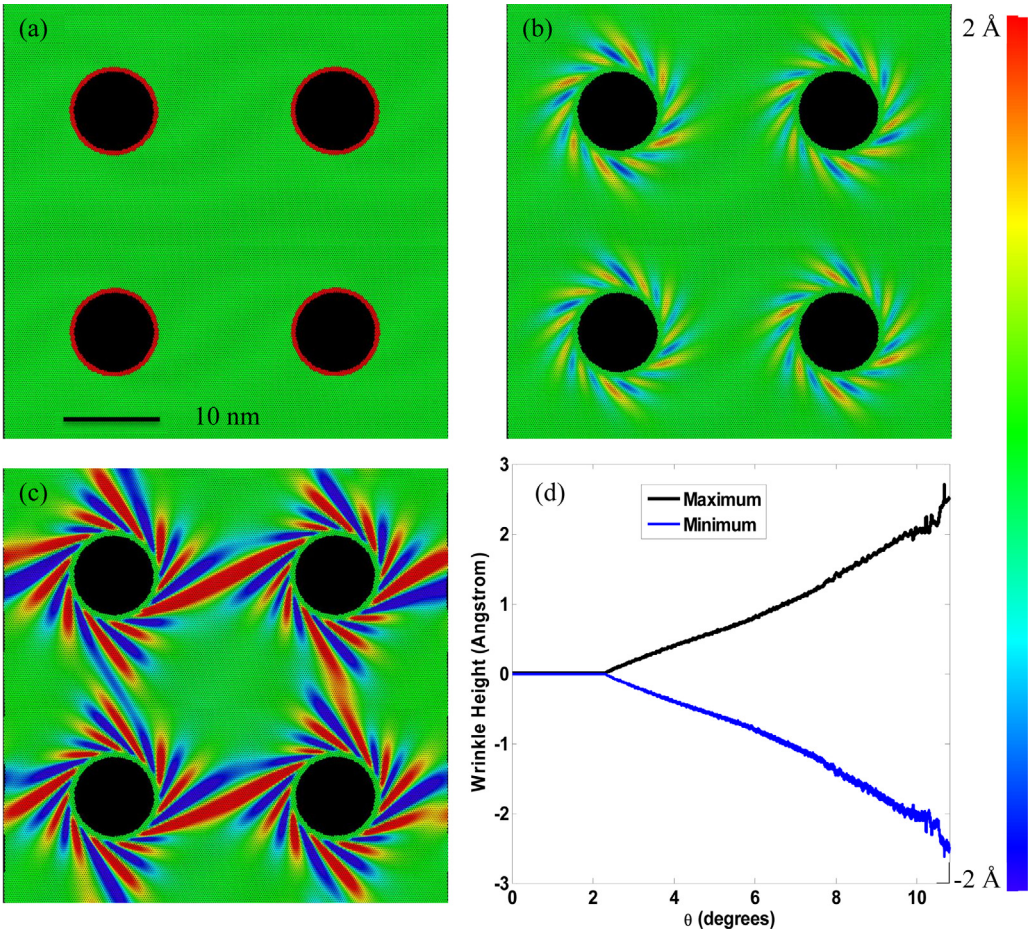

Fig. 1. The setup is shown in (a); the red regions are fixed and a fixed-period rotation is applied to them in either a clockwise or anticlockwise direction (scale bar is 10 nm). The initiation of wrinkling at 2.7° is shown in (b), and the second-stage wrinkle pattern at 9.5° is shown in (c). The upper and lower bounds for the *z*-displacement are shown in (d). For (b) and (d), the scale bar is shown to the right. For subsequent figures, *z*-displacement is scaled to this same bar. (For interpretation of the references to color in this figure legend, the reader is referred to the web version of the article.)

where $V_{ij}^{\mathrm{R}}(r_{ij})$ is a repulsive term, $V_{ij}^{\mathrm{A}}(r_{ij})$ is an attractive term, and b_{ij} is the environmental-dependent bond order term between atoms which activates the attractive term only for bonded atoms. The AIREBO potential is best suited for systems of hydrogen and carbon, rendering the all-carbon system presented here well defined [37]. As the REBO potential only accounts for interactions of atoms within two Angstroms of one another, the AIREBO potential also includes the E_{ij}^{LJ} term, which is a standard 12-6 Lennard–Jones potential for distances past a 2 Å limit. The cutoff for the LJ term is set here to be 10.2 Å as a good balance between computation speed and accuracy. The AIREBO potential also includes the $E_{kijl}^{\mathrm{TORSION}}$ term, which is a four-body potential describing hydrocarbon dihedral angle preference. The AIREBO potential has previously been used successfully in studying the properties of various carbon allotropes, especially including graphene [43–48].

As seen in Fig. 1(a), the system is a sheet of graphene concurrent with the *x*–*y* plane of size 50 nm in both the *x* and *y* directions. The entire system is periodic in the *x* and *y* directions, and is minimized before being controlled at 1 K with NVT ensemble. While the system is kept at 1 K to demonstrate the patterns more clearly, the patterns are also observable at higher temperatures, as can be seen from Fig. S1 of the Supplementary Material. Four holes are created at equally spaced intervals of radius 5 nm, unless otherwise specified. The atoms of the hole are removed, except for the 0.5 nm outer strip, through which a fixed-period rotation is applied. The atoms adjacent to the hole are fixed, so that there is no effect on the remainder of the sheet from the 'dangling bonds' at the edges of the holes. These 'holes' are created to provide an easy visualization of the torqued areas, and to show that these patterns can be created by twisting attached CNTs or other objects embedded in a graphene sheet.

A rotation is applied in either the clockwise (here denoted as 1) or anticlockwise (here denoted as 2) direction, with the pattern of twisting labeled clockwise from the bottom-left hole (1111, 1112, 1122, and 1212). It is assumed in this work that the direction of rotation is only remarkable in relation to nearby rotations, as symmetry is assumed in the case of the graphene sheet. Thus the four rotational patterns are chosen to be distinct from each other while taking symmetry into account. In order to maintain a slow and stable rotation, the rotation velocity of any hole is chosen as 1°/ns, unless otherwise mentioned. For determining the effects of torsion velocity, the '1' holes in pattern 1122 are kept at a constant speed while the '2' holes are rotated at a speed relatively slower or faster. For determining the effects of hole size, the '1' holes in pattern 1212 are increased in 5 Angstrom increments while the '2' holes are diminished by an amount which keeps the total hole area the same. The total hole area is kept constant in order to keep the area of the free graphene sheet constant, so that each pattern has the same number of atoms in the wrinkling area. To show comparisons, Fig. S2 of the Supplementary Material shows some wrinkling patterns for two patterns of double total hole area.